

Demixing Phase Transition in a Mixture of Hard-Sphere Dipoles and Neutral Hard Spheres

X. S. Chen, M. Kasch, and F. Forstmann

Institut für Theoretische Physik, Freie Universität Berlin, Arnimallee 14, 1 Berlin 33, Germany

(Received 12 June 1991)

For a mixture of hard-sphere dipoles and neutral hard spheres we calculate the correlation functions from integral equations and evaluate the concentration structure factor $S_{cc}(k)$. For large enough dipolar interaction, this structure factor becomes infinite, indicating a demixing phase transition. This instability is also found for charged hard spheres in a dipolar solvent and is the reason for the problems faced previously in investigations of hard-sphere model electrolytes.

PACS numbers: 61.20.Gy, 64.70.Ja, 82.60.Lf

Mixtures of hard-sphere dipoles and hard-sphere ions are studied as models of electrolytes. They are theoretically investigated by simulations [1–3] and by Ornstein-Zernike-type integral equations [4–6]. With both approaches, unsurmountable difficulties appeared when interesting concentration ranges, e.g., 1M solutions of singly charged ions, were studied. Only wild guesses for the reasons for this desperate situation were discussed, especially questioning the approximations in the theory.

We have now discovered that a demixing phase transition of the system is the reason for the unsatisfactory answers in studies that start from the expectation that the system is homogeneous.

We demonstrate in this Letter the capability of the Ornstein-Zernike integral equations with a reference hypernetted chain closure (RHNC) to analyze the demixing phase transition. The detailed calculation is for the simpler system with no charge on the hard spheres,

which are dissolved in the dipolar hard spheres. We have seen the same phase transition for a 1.5M solute of charged hard spheres, when the charge grows to a value of about $\frac{2}{3}$ of an electron charge in the same dipolar solvent as studied here.

1. Susceptibilities.—The demixing phase transition is seen by a singularity in a susceptibility. We first derive the relations between several susceptibilities and the correlation functions calculable from the integral equations.

In view of the experimental conditions, fluctuations are usually considered at constant pressure [7,8]. In the integral equations the independent variables defining the system are the particle densities, not the pressure or the partial pressures. Therefore the density-functional expansion of the grand free energy is the proper starting point for relating the susceptibilities to the correlation functions:

$$\Omega[T, \rho_\alpha + \delta\rho_\alpha] = \Omega[T, \rho_\alpha] + \frac{1}{2} \int \int \sum_{\alpha\beta} \frac{\delta\Omega}{\delta\rho_\alpha(1)\delta\rho_\beta(2)} \Big|_{\text{equilib}} \delta\rho_\alpha(1)\delta\rho_\beta(2) d1 d2. \quad (1)$$

The second functional derivatives of Ω are related to the direct correlation functions [9–11]:

$$\frac{\delta^2\Omega}{\delta\rho_\alpha(1)\delta\rho_\beta(2)} \Big|_{\text{equilib}} = kT \left[\frac{\delta_{\alpha\beta}\delta(1,2)}{\rho_\alpha(1)} - c_{\alpha\beta}(1,2) \right]. \quad (2)$$

The variables $1 \equiv (\mathbf{r}_1, \omega_1)$ imply the position and orientation of particles, e.g., dipoles, and $\rho_\alpha(1)$ gives the number of particles α at \mathbf{r}_1 pointing in the direction ω_1 per unit volume and unit space angle. $\rho_\alpha(\mathbf{r}_1) = \int d\omega_1 \rho_\alpha(1)$ is the number density per unit volume; for the homogeneous system we write ρ_α . $\delta\rho_\alpha(1)$ as well as the correlation

functions $c_{\alpha\beta}(1,2)$ are expanded in spherical harmonics:

$$\delta\rho_\alpha(1) = \sum_{lm} \delta\rho_\alpha^{lm}(\mathbf{r}_1) Y_{lm}(\omega_1), \quad (3)$$

$$c_{\alpha\beta}(1,2) = \sum_{l_1 l_2} c_{\alpha\beta}^{l_1 l_2}(\mathbf{r}_{12}) \Phi^{l_1 l_2}(\omega_1 \omega_2 \omega_r). \quad (4)$$

The functions $\Phi^{l_1 l_2}(\omega_1 \omega_2 \omega_r)$ are linear combinations of spherical harmonics, the so-called spherical invariants [12,13]. The integrals in Eq. (1) are convolutions, and become products when being Fourier transformed. After the angle integration and the so-called “**k**-frame” transformation [12,13] we obtain

$$\delta\Omega = \frac{kT}{2} \frac{1}{(2\pi)^3} \int d^3k \sum_m \sum_{\alpha\beta} \sum_{l_1 l_2} 4\pi \delta\tilde{\rho}_\alpha^{l_1 m}(k) \rho_\alpha^{-1/2} \times [\delta_{\alpha\beta} \delta_{l_1 l_2} - (-1)^m c_{\alpha\beta}^{l_1 l_2 m}(k) \rho_\alpha^{1/2} \rho_\beta^{1/2} (2l_1 + 1)^{-1/2} (2l_2 + 1)^{-1/2}] \rho_\beta^{-1/2} \delta\tilde{\rho}_\beta^{l_2 m}(k)^*. \quad (5)$$

Defining a vector $\delta\tilde{\rho}(m, k)$, a diagonal matrix $\rho^{-1/2}$, and the bracket in Eq. (5) as the matrix $\mathbf{I} - (-1)^m \tilde{\mathbf{C}}(m, k)$, Eq. (5) can be rewritten as

$$\delta\Omega = \frac{kT}{2} \int d^3k \sum_m 4\pi \delta\tilde{\rho}(m, k) \rho^{-1/2} [\mathbf{I} - (-1)^m \tilde{\mathbf{C}}(m, k)] \rho^{-1/2} \delta\tilde{\rho}^\dagger(m, k). \quad (6)$$

The indices of a vector and matrix denote kinds of particles as well as angular indices from the expansions in Eqs. (3) and (4). Details can be found in Ref. [14]. In Eqs. (5) and (6) $\delta\Omega$ appears as a homogeneous polynomial of degree 2 in the density fluctuations introduced in Eq. (3). The coefficients forming the matrix $\tilde{\mathbf{C}}$ are calculated from the direct correlation functions $c_{\alpha\beta}^{l_1 l_2 l}(\mathbf{r}_{12})$.

For our discussion in this paper we are interested only in the $m=0$ part of Eq. (6). $m \neq 0$ parts relate to the polarization fluctuation and multipole moment fluctuations. When we include in the expansion Eqs. (3) and (4) $l_1, l_2 \leq 3$, $\mathbf{I} - \tilde{\mathbf{C}}(m=0, k)$ is a 5×5 matrix and has block diagonal form. The particle densities are related to a 3×3 submatrix $[\mathbf{I} - \tilde{\mathbf{C}}(0, k)]_3$, with the indices 1 = (neutral), 2 = (dipole, $l=0, m=0$), 3 = (dipole, $l=2, m=0$). In a complete analysis [15], we should diagonalize this matrix and search for the smallest eigenvalue, which goes to zero, and study the corresponding eigenvector. As a shortcut, we have calculated $\text{Det}[\mathbf{I} - \tilde{\mathbf{C}}(0, k)]_3$. This is the denominator in the concentration-concentration structure factor

$$S_{cc}(k) = \frac{1}{N} \langle \delta\tilde{c}(k) \delta\tilde{c}(-k) \rangle = \frac{(1/N) \int \delta\tilde{c}(k) \delta\tilde{c}(-k) e^{-\beta\delta\Omega}}{\int e^{-\beta\delta\Omega}}. \quad (7)$$

The concentration is defined as $c(\mathbf{r}_1) = \rho_d(\mathbf{r}_1)/\rho(\mathbf{r}_1)$, and $\rho(\mathbf{r}_1) = \rho_d(\mathbf{r}_1) + \rho_n(\mathbf{r}_1)$; for the homogeneous system we write c and ρ . Therefore $\delta\tilde{c}(k) = \rho^{-1}[(1-c)\delta\tilde{\rho}_d(k) - c\delta\tilde{\rho}_n(k)]$. Using Eq. (6) and the technique outlined in Ref. [16] we have

$$S_{cc}(k) = \frac{c(1-c)[\alpha_{11}(k)\alpha_{33}(k) - \alpha_{13}^2(k)]}{\text{Det}[\mathbf{I} - \tilde{\mathbf{C}}(0, k)]_3}, \quad (8)$$

where

$$\alpha_{11}(k) = 1 - \rho[(1-c)^2 \tilde{c}_{nn}^{000}(k) + 2c(1-c) \tilde{c}_{nd}^{000}(k) + c^2 \tilde{c}_{dd}^{000}(k)],$$

$$\alpha_{33}(k) = 1 - \rho_d \tilde{c}_{dd}^{220}(k)/5,$$

and

$$\alpha_{13}(k) = (\rho_d \rho / 5)^{1/2} [(1-c) \tilde{c}_{nd}^{020}(k) + c \tilde{c}_{dd}^{020}(k)].$$

Using the Ornstein-Zernike equation $S_{cc}(k)$ can also be expressed by the total correlation functions $h_{\alpha\beta}(1, 2)$:

$$S_{cc}(k) = c(1-c) \{ 1 - \rho [(1-c)^2 \tilde{h}_{nn}^{000}(k) + 2c(1-c) \tilde{h}_{nd}^{000}(k) + c^2 \tilde{h}_{dd}^{000}(k)] \}. \quad (9)$$

When there is no interaction between the particles, then $S_{cc}(k) = S_{cc}^{id} = c(1-c)$.

2. Demonstration of the phase transition.—Our system contains hard spheres of diameter σ with dipoles in their center (the solvent) and neutral hard spheres of the same

diameter σ (the solute). The strength of the dipole interaction is characterized by $\mu^{*2} = \mu^2/\sigma^3 kT$, with dipole moment μ and temperature T . The reduced density of the whole mixture is $\rho^* = \rho\sigma^3 = 0.8$. We vary the concentration of solvent c . The correlation functions $c_{ij}(1, 2)$ are calculated from the Ornstein-Zernike equation,

$$h_{\alpha\beta}(1, 2) = c_{\alpha\beta}(1, 2) + \sum_{\gamma} \int h_{\alpha\gamma}(1, 3) \rho_{\gamma}(3) c_{\gamma\beta}(3, 2) d3, \quad (10)$$

and the RHNC closure [17],

$$1 + h_{\alpha\beta}(1, 2) = \exp[-\beta u_{\alpha\beta}(1, 2) + h_{\alpha\beta}(1, 2) - c_{\alpha\beta}(1, 2) + B_{\alpha\beta}(1, 2)], \quad (11)$$

where $u_{\alpha\beta}(1, 2)$ is the interaction potential between particles α at 1 and β at 2, and the ‘‘bridge term’’ $B_{\alpha\beta}(1, 2)$ is chosen such that the known pure-hard-sphere result [18, 19] is obtained when the dipoles are switched off:

$$B_{\alpha\beta}(1, 2) = \ln[1 + h_{\alpha\beta}^{\text{hs}}(1, 2)] - h_{\alpha\beta}^{\text{hs}}(1, 2) + c_{\alpha\beta}^{\text{hs}}(1, 2). \quad (12)$$

Comparison with simulations [1, 4] has shown that Eqs. (10)–(12) yield good correlation functions for ion-dipole mixtures. The angular functions are again expanded in spherical invariants and Eqs. (10) and (11) yield a system of integral equations for the r -dependent expansion coefficients, which is solved by iteration. If the angular expansion includes $l_1, l_2 \leq 3$, we have 19 unknown functions. The solution procedure is similar to that published by Fries and Patey [4] combined with the ideas of Caillol [20]. Details will be published elsewhere [15].

When the iterative process has converged, we take the direct correlation functions $c_{ij}(1, 2)$ and evaluate the susceptibility Eq. (8). For the dipole strength μ^{*2} between 2.1 and 2.6 we plot the smallest value of $S_{cc}^{id}/S_{cc}(k)$, which turns out to be at $k=0$, versus dipole concentration c in Fig. 1.

The zeros of $S_{cc}^{-1}(k)$ in Fig. 1 indicate the demixing phase transition. The closer we come to the phase transition the more difficult it becomes to find convergent solutions of the iteration process. The drop to zero appears to be rather sudden. We have extrapolated to the zeros in Fig. 1 and plotted a phase diagram in Fig. 2. The curve in the phase diagram separates the homogeneous phase below from the unstable phase above. It is a spinodal. Further investigations are necessary to find the coexistence curve. We have checked that curtailing the angular expansions at an earlier stage ($l_1, l_2 \leq 2$) makes only small numerical but no qualitative differences.

3. Demixing of ion solutions.—We have found the same instability for hard-sphere ions dissolved in hard-sphere dipoles. We investigated a 1.5M ionic solution ($\rho_+^* = \rho_-^* = 0.056655$) in a solvent of density $\rho_d^* = 0.8$ and $\mu^{*2} = 2.0$. We gradually increased the charge on the positive as well as on the negative ions. The charge is measured by $q^{*2} = q^2/\sigma kT$, where q is the charge of one ion.

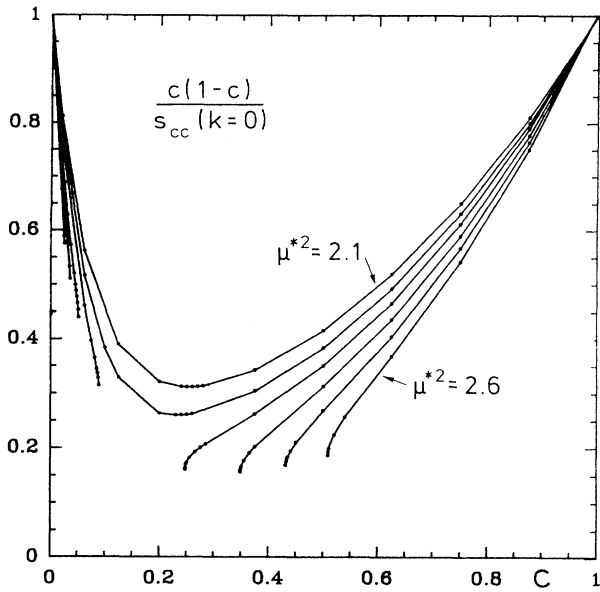


FIG. 1. The inverse structure factor $c(1-c)S_{cc}^{-1}(k=0)$ vs dipole concentration c for several values of dipole interaction $\mu^{*2}=2.1, 2.2, \dots, 2.6$.

When q^{*2} grows to 57.0, a demixing instability occurs, again demonstrated by a zero in the denominator of the concentration-concentration structure factor $S_{cc}(k)$ analogous to Eq. (8). If the ionic density is decreased to $1M$ ($\rho_+^* = \rho_-^* = 0.03777$), the transition occurs at higher ionic charge, close to $q^{*2} = 60$. For very small ionic densities like $10^{-7}M$ there is no instability up to $q^{*2} = 144$ (corresponding to one electron charge on the ion at room temperature and $\sigma \approx 4 \text{ \AA}$). Many more calculations are necessary to yield a phase diagram, but we can say already that with lower ionic charge we can go to higher ionic concentrations before the instability occurs.

4. *Inside the spinodal region.*—What happens when we try to determine the correlation functions inside the spinodal region? With the same iterative program it is actually possible to find convergent correlation functions in this region which have a long-range oscillating tail with a wavelength much larger and not necessarily a multiple of the particle diameter σ , contrary to the fast-decaying correlation functions outside the spinodal range. Examples are shown in Fig. 3, which is for the case $\mu^{*2} = 2.0, q^{*2} = 58.0, \rho_d^* = 0.8, \rho_+^* = \rho_-^* = 0.056655$. Because $\rho_{\beta} g_{\alpha\beta}(1,2) = \rho_{\beta} [1 + h_{\alpha\beta}(1,2)]$ is the density of particles of kind β at 2 under the condition that there is a particle α at 1, the content of Fig. 3 can be read as follows: Around a particle (ion or dipole) there are shells of alternating concentrations of ions and dipoles. The ion concentration wave is in phase for + and - ions yielding shells which are locally neutral. Only the neighboring three shells of particles do the screening. The wave of the dipole concentration is half a wavelength out of phase

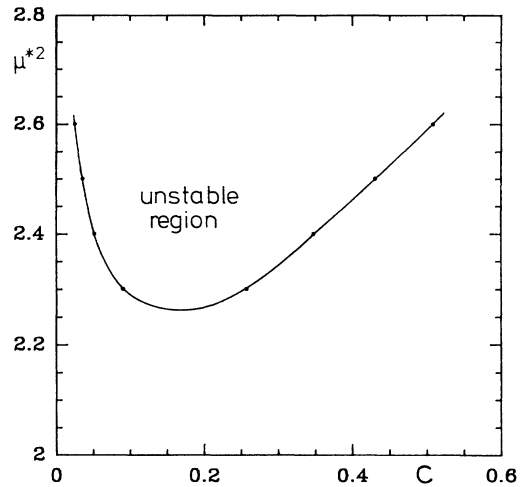


FIG. 2. Phase diagram for a mixture of hard-sphere dipoles and neutral hard spheres. The spinodal line separates the unstable region from the stable or metastable region.

compared to that of the ions. Their maximal density fills in the minima of the ion density to such perfection that the particle density shows no long-range oscillations as in a normal liquid. The constancy of particle density and the neutralization of charge can be seen from the condi-

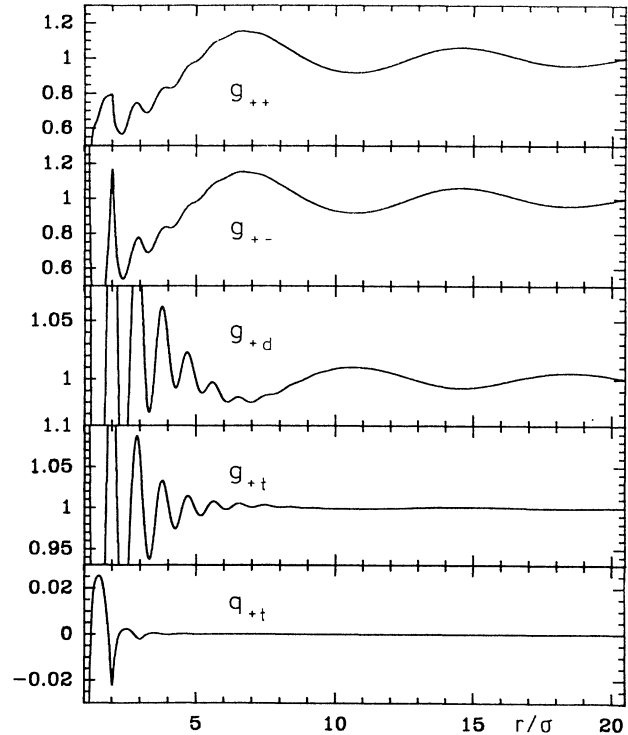


FIG. 3. A solution inside the spinodal region, and the correlations around a positive ion. The last two curves show the conditional local total density and the local total charge density.

tional local total density

$$(\rho_+ + \rho_- + \rho_d)g_{+l}(1,2)$$

$$= \rho_+g_{++}(1,2) + \rho_-g_{+-}(1,2) + \rho_dg_{+d}(1,2)$$

and the conditional local total charge density $qq_{+l}(1,2) = q[\rho_+g_{++}(1,2) - \rho_-g_{+-}(1,2)]$, which are plotted as the last two curves in Fig. 3. We find that with these correlation functions, the denominator of the structure factor has a zero at exactly that k value which belongs to the long-range concentration waves. The related singularity is integrable. Because Eqs. (10) and (11) can be derived (with some approximation) from the requirement that the grand free energy is stationary with respect to variations in local particle density, we come to the interpretation that we find at least metastable states with concentration waves in the spinodal region. Because we asked for conditional densities in an infinite system, we see the concentration waves around our particle, which is at the center and breaks the translational symmetry. In a finite system, as could be simulated for instance, one should find the concentration waves normal to the boundaries. Exactly analogous circumstances have recently been found experimentally in a case of spinodal decomposition [21], though in that case, the state with the concentration waves slowly degraded to longer wavelengths. In further studies we hope to analyze the degree of metastability of our state with concentration waves.

Conclusions.— We have discovered a demixing phase transition in a mixture of hard-sphere dipoles with hard-sphere ions or neutral hard spheres of equal size. In the case of neutral solute the phase transition requires a minimal strength of the dipole interaction μ^{*2} . For larger dipole moments (lower temperature), the spinodal region grows. With ions dissolved in the dipoles, rather small concentrations such as $1M$ or $1.5M$ show demixing, when the charge on the ions q^{*2} grows to a certain value. This instability is the reason for previous problems with integral equations and simulations investigating the hard-sphere model electrolyte. Inside the spinodal region, there appear to be at least metastable states with concentration waves. Indications of a demixing tendency have been reported in a Monte Carlo simulation [3] which has too many limitations to be conclusive. The driving force for the demixing is obviously a lowering of the dipole interaction energy when the dipoles can optimize their ar-

angement, not being disturbed by the wrong concentration of nondipoles. This mechanism reminds one of the expulsion of “hydrophobic” molecules from water. There the optimization of a hydrogen bond network is the driving mechanism. We would like to be informed about miscibility gaps in chemical systems which come close to hard-sphere dipoles and equal-size ions.

-
- [1] J. M. Caillol, D. Levesque, and J.J. Weis, *Mol. Phys.* **69**, 199 (1990).
 - [2] K. Y. Chan, K. E. Gubbins, D. Henderson, and L. Blum, *Mol. Phys.* **66**, 299 (1989).
 - [3] J. Eggebrecht and P. Ozler, *J. Chem. Phys.* **93**, 2004 (1990).
 - [4] P. H. Fries and G. N. Patey, *J. Chem. Phys.* **82**, 429 (1985).
 - [5] W. Dong, M. L. Rosinberg, A. Perera, and G. N. Patey, *J. Chem. Phys.* **89**, 4994 (1988).
 - [6] D. Levesque, J. J. Weis, and G. N. Patey, *J. Chem. Phys.* **72**, 1887 (1980).
 - [7] T. Biben and J. P. Hansen, *Phys. Rev. Lett.* **66**, 2215 (1991).
 - [8] A. B. Bhatia and D. E. Thornton, *Phys. Rev. B* **2**, 3004 (1970).
 - [9] N. D. Mermin, *Phys. Rev.* **137**, 1441 (1965).
 - [10] J. L. Lebowitz and J. K. Percus, *J. Math. Phys.* **4**, 116 (1963).
 - [11] W. F. Saam and C. Ebner, *Phys. Rev. A* **15**, 2566 (1977).
 - [12] L. Blum and A. J. Torruella, *J. Chem. Phys.* **56**, 303 (1972).
 - [13] C. G. Gray and K. E. Gubbins, *Theory of Molecular Fluids* (Oxford Univ. Press, London, 1984), Vol. 1.
 - [14] X. S. Chen, F. Forstmann, and M. Kasch, *J. Chem. Phys.* (to be published).
 - [15] X. S. Chen, F. Forstmann, and M. Kasch (to be published).
 - [16] L. D. Landau and E. M. Lifshitz, *Statistical Physics* (Pergamon, New York, 1980), 3rd ed., Pt. 1.
 - [17] F. Lado, *Phys. Rev. A* **135**, 1013 (1964); *Mol. Phys.* **31**, 1117 (1976).
 - [18] L. Verlet and J. J. Weis, *Phys. Rev. A* **5**, 939 (1972).
 - [19] D. Henderson and E. W. Grundke, *J. Chem. Phys.* **63**, 601 (1975).
 - [20] J. M. Caillol, *Chem. Phys. Lett.* **121**, 347 (1985); **156**, 357 (1989).
 - [21] R. A. L. Jones, L. J. Norton, E. J. Kramer, F. S. Bates, and P. Wiltzius, *Phys. Rev. Lett.* **66**, 1326 (1991).